ACS OMEGA

http://pubs.acs.org/journal/acsodf
Article

Surface-Enhanced Raman Scattering (SERS) in Combination with PCA and PLS-DA for the Evaluation of Antibacterial Activity of 1-Isopentyl-3-pentyl-1*H*-imidazole-3-ium Bromide against *Bacillus subtilis*

Fatima Tahir,[#] Ali Kamran,[#] Muhammad Irfan Majeed,[*] Abeer Ahmed Alghamdi,[*] Muhammad Rizwan Javed, Haq Nawaz,[*] Muhammad Adnan Iqbal, Muhammad Tahir, Anam Tariq, Nosheen Rashid, Urwa Shahid, Ahmad Hassan, and Umar Sohail Shoukat

Cite This: *ACS Omega* 2024, 9, 6861−6872

Read Online

ACCESS | Metrics & More | Article Recommendations | Supporting Information

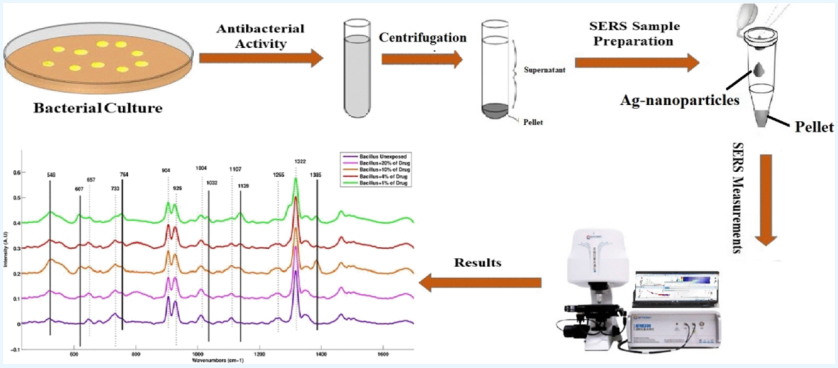

ABSTRACT: In the current study, surface-enhanced Raman scattering (SERS) was performed to evaluate the antibacterial activity of lab-synthesized drug (1-isopentyl-3-pentyl-1*H*-imidazole-3-ium bromide salt) and commercial drug tinidazole against*Bacillus subtilis*. The changes in SERS spectral features were studied for unexposed bacillus and exposed one with various dosages of drug synthesized in the lab (1-isopentyl-3-pentyl-1*H*-imidazole-3-ium bromide salt), and SERS bands were assigned associated with the drug-induced biochemical alterations in bacteria. Multivariate data analysis tools including principal component analysis (PCA) and partial least-squares discriminant analysis (PLS-DA) have been utilized to analyze the antibacterial activity of the imidazole derivative (lab drug). PCA was employed in differentiating all the SERS spectral data sets associated with the various doses of the lab-synthesized drug. There is clear discrimination among the spectral data sets of a bacterial strain treated with different concentrations of the drug, which are analyzed by PLS-DA with 86% area under the curve in receiver operating curve (ROC), 99% sensitivity, 100% accuracy, and 98% specificity. Various dominant spectral features are observed with a gradual increase in the different concentrations of the applied drug including 715, 850, 1002, 1132, 1237, 1396, 1416, and 1453 cm^{-1}, which indicate the possible biochemical changes caused in bacteria during the antibacterial activity of the lab-synthesized drug. Overall, the findings show that imidazole and imidazolium compounds generated from tinidazole with various alkyl lengths in the amide substitution can be effective antibacterial agents with low cytotoxicity in humans, and these results indicate the efficiency of SERS in pharmaceuticals and biomedical applications.

1. INTRODUCTION

Antibiotics are mainly used to cure various bacterial infections and diseases, but misuse and overdosage of antibiotics have led to several multidrug-resistant bacteria. Antibiotic resistance traits have spread widely, rendering antibiotics ineffective and posing major economic and health risks.[1,2] The spread and propagation of antibiotic resistance can be slowed down and even stopped with the rapid detection of resistant strains and by treatment with an effective dosage of the drug. Different conventional approaches such as disk diffusion, microdilution, and gradient disk diffusion methods were employed for the detection and assessment of antibiotic-sensitive and resistant microorganisms are time-consuming.[3,4]

Received: October 18, 2023
Revised: January 5, 2024
Accepted: January 16, 2024
Published: January 30, 2024

https://doi.org/10.1021/acsomega.3c08196
ACS Omega 2024, 9, 6861−6872

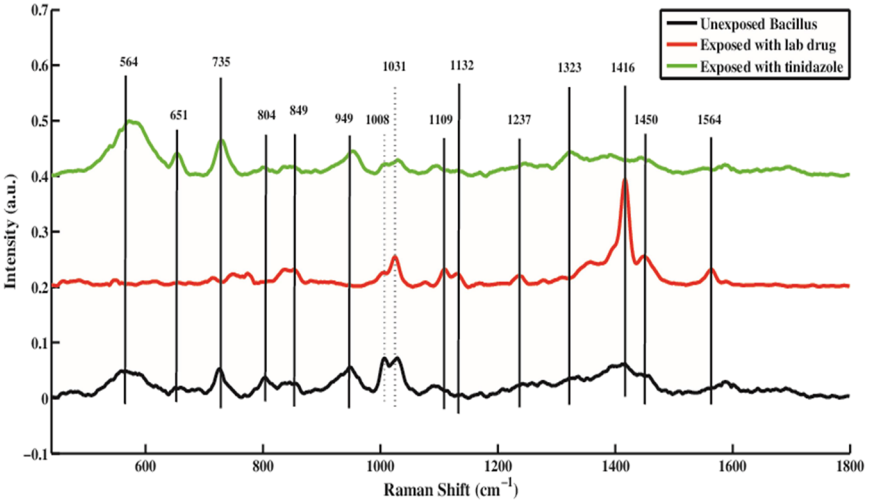

Figure 1. Mean SERS spectra of untreated *Bacillus subtilis* and exposure of *Bacillus subtilis* to lab drug and tinidazole.

N-Heterocyclic carbenes (NHC) are even more versatile than phosphines and have been regarded as building block ligands. NHC's extraordinary and unique characteristics, such as being strong σ-electron donors that make them effective ligands, have influenced the study of coordination and organometallic chemistry. These properties can be modified based on the *N*-substituents.[5] This is because the NHC precursors (in the form of imidazolium salts) were found to be stable to air and moisture. The NHC-carbenes have been applied in the field of medicine as therapeutic agents depending upon their biological activity, which includes but is not limited to, antimicrobial, antiviral, antifungal, and anticancer.[6] The substituted imidazolium compounds are found to show activity against pathogenic bacteria. Even if the exact process causing bacterial cell damage is still not fully understood, several hypotheses are reported in the literature, and the most important is that the lipophilicity of these compounds causes a change in membrane permeability. The lipophilicity is increased by the bulky substituents, which leads to enhance their antimicrobial potential.[7]

Different aromatic heterocyclic compounds have been employed for a variety of bioactive chemicals including antimicrobials, antifungal, anticancer, and antidiabetic agents.[8−10] In medicinal chemistry, the search for novel and powerful imidazole-derived bioactive drugs continues to be a major focus.[11,12] For medical purposes, imidazole and its derivatives are often utilized. For medical purposes, imidazole and its derivatives are often utilized as antibiotics,[13] antifungal,[14] and anticancerous.[15]

Antibacterial drugs based on imidazole and imidazolium derivative salts have been investigated against *Bacillus spp.*[16,17] for causing a number of harmful infections such as osteomyelitis, meningitis, anthrax, endocarditis, and ophthalmitis.[18] High antibacterial activity of imidazolium salts based on amino acids has been demonstrated in the literature.[19,20] *Bacillus spp.* cause several diseases in humans and other organisms, so it is a major concern of research nowadays in order to develop new antibiotics.[17,21]

The imidazolium skeleton can be converted into ionic liquids with intriguing pharmacological effects in this regard.[22,23] Tinidazole is also studied in the literature for its antibacterial activity.[17,21] It is a 5-nitroimidazole and in anaerobes, it is intracellularly reduced to active intermediates that interact with nucleic acids to induce instability and breakage. With a half-life (12−14 h), which is twice that of metronidazole, tinidazole is antimicrobial against anaerobic bacteria.[24]

The discovery of novel antibiotics against bacteria can benefit from a research investigation exploring the metabolic mechanisms of potential drug candidates' antibacterial action. For the analysis of antibacterial activity, a variety of analytical techniques are used, including imaging. Scanning electron microscopy (SEM), confocal imaging, and transmission electron microscopy (TEM) are examples of imaging techniques. These techniques clearly show the bacterial cell damage followed by the exposure to drugs and antibiotics, but they are not able to reveal the mechanism of action or the biochemical alterations which take place after antibiotic exposure.[25]

The spectro-analytical techniques like mass spectrometry (MS), Fourier transform infrared spectroscopy (FT-IR), nuclear magnetic resonance (NMR), and fluorescence spectroscopy approaches can indicate metabolic alterations inside the cells, but they need substantial sample preparation. Raman scattering and its modality called surface-enhanced Raman scattering (SERS) have great potential to analyze the fingerprint spectra of biomolecules. SERS has demonstrated to be an attractive analytical approach and their interaction with different drug candidates is used in the research of biological systems, especially in the characterization and identification of bacteria.[14,22]

The purpose of this research is to develop a SERS approach for directly determining lab-synthesized and commercial drug (tinidazole) antibiotic sensitivity toward bacterium by detecting the biochemical alterations in bacteria after their interaction with the antibiotic. Silver nanoparticles (NPs) can improve and enhance the Raman spectral features of biomolecules, resulting in bacterial "fingerprints".[26−28] According to the electromagnetic mechanism, a stronger resonance enhancement effect will be produced by nanoparticles with high absorption at the excitation wavelength compared to those with insignificant absorption.[29]

As the bacteria interact with different antibiotics, the acquired SERS signals from the bacterial cell may be utilized to demonstrate the biochemical alterations caused by the drug. Studying metabolic/biochemical alterations induced by anti-

https://doi.org/10.1021/acsomega.3c08196
ACS Omega 2024, 9, 6861−6872

biotics may help us to understand bacterial cell responses to antibiotic treatments and estimate bacterial cell susceptibility.[30−32] Moreover, chemometric tools such as PCA and PLS-DA were applied to find out the antibacterial activity of the lab-synthesized imidazolium salt.

This study proposes a quick and easy SERS approach to determine induced biochemical changes in *Bacillus subtilis* caused by the exposure of different concentrations of the laboratory-synthesized imidazole derivative in comparison to the market-available tinidazole. Both these drug candidates are imidazole derivatives that have medicinal applications and somewhat have different modes of action that are compared and studied thoroughly in this report.

2. RESULTS AND DISCUSSION

SERS spectra for all samples were recorded and then MATLAB R2009a (The MathWorks, USA) was used for preprocessing of all these raw spectra, and the multivariate data analysis and mean spectral analysis proceeded next. Figure 1 represents the mean SERS spectra of untreated *Bacillus subtilis* (black), treated with lab drug (red) and with the market-available drug tinidazole (green), in which vertical lines show differentiating spectral features. These are explained and summarized in Table 1 along with the proper assignments, and corresponding literature citations are also added. Raman spectra were collected for unexposed bacillus and bacillus exposed to different concentrations of in-house-synthesized and market-available drug tinidazole. Changes in the bacteria's cell wall and structure were linked to changes in SERS spectral features. Numerous different types of biomolecules are present in bacterial cells. resulting in a distinct SERS spectrum.

Table 1. SERS Assignments for *Bacillus subtilis*

Raman shift/ cm^{-1}	assignment/biomolecules	component	reference
564	(C_S_S_C) vibration in proteins	protein	33,34
597	phosphatidylinositol	phospholipids	35
651	NH deformation of amide- II	protein	34
715	C−N stretching	protein	36,37
726	adenine/DNA	DNA	10,36
735	adenine/nucleic acid	DNA	37,38
749	nucleic acid component	DNA	39
804	uracil-based ring breathing mode	DNA	40
850	C−O−C stretching in 1,4-glycosidic link	carbohydrates	40,41
949	most likely as a result of single bond stretching vibrations in polysaccharides, proline, and valine amino acids	protein and polysaccharides	40
1002−1004	C−C aromatic ring stretching (phenylalanine)	protein	42−44
1008	C−C aromatic ring breathing of Phe	protein	45
1031	C−O stretching band of glycosidic bond, polysaccharides	carbohydrates	40
1109	carbohydrates band for solution	carbohydrates	46
1132	unsaturated fatty acid	lipids	43,47
1237	amide III and CH2 wagging vibrations from glycine backbone and proline side chains	protein	40,48
1270	amide-III	protein	26
1323	C−H bend in protein	protein	42
1396	*N*-acetylglucosamine	protein	49
1416	tryptophan	protein	19
1450	CH_2 bending, C−H deformation,	protein and carbohydrates	37,42
1564	N−H bending	protein	50

The SERS bands differentiating unexposed bacillus and bacillus exposed to the drug are shown by solid lines, while the characteristics associated with intensity changes observed in all are shown by dotted lines. The relatively comparable features found in both mean spectra of unexposed and exposed bacteria indicate the chemical structural similarity between tinidazole and imidazole derivative (lab-synthesized drug) and their interaction with Bacillus bacteria. The noticeable variations can be directly related to the breakdown of the bacterial cell structure. The intensity differences and shifts in bands in these mean spectra indicate the biochemical changes in bacteria caused by in-house-synthesized drugs and tinidazole.

The majority of the biological composition of a bacteria includes nucleic acids (DNA and RNA), proteins (amino acids), lipids, polysaccharides, and inorganic ions.[51] In the case of Gram-positive bacteria,[26] its origin is attributed to glycosidic ring vibrations which arise due to the bacterial cell wall's polysaccharide components. Gram-positive bacteria possess a thick layer of peptidoglycan in their cell walls, which is made up of *N*-acetyl-D-glucosamine and *N*-acetylmuramic acid linked by peptide bridges. Phospholipids are covered by a peptidoglycan layer and protein-rich cytoplasmic membrane, which may also contain a coating of proteins organized in a para-crystalline structure (S-layer).[34]

The SERS features at 735 cm^{-1} (adenine) and 804 cm^{-1} (uracil ring breathing) are linked with the nucleus of the bacterial cell, which is found diminished in intensity after the exposure of the lab-synthesized drug in comparison to commercial drug tinidazole. This decrease in SERS features showed that lab drug damaged the bacterial DNA and RNA. The distinct features in the mean SERS spectra at 564 cm^{-1} (C−S−S-C vibrational mode) associated with disulfide bonds indicate the stabilization and normal functioning of proteins. These are nearly always present in bacteria, but their concentrations can vary, therefore the strength of the SERS signal can alter depending on the species. This diminishing in the intensity of the broad SERS band at 564 cm^{-1} due to exposure to the lab-synthesized drug might be due to the degradation or disintegration of proteins present.[49] SERS band at 651 cm^{-1} (N−H deformation of amide-II), 949 cm^{-1} (single bond stretching vibrations for the amino acids and polysaccharides), 1008 cm^{-1} (C−C aromatic ring breathing of Phenylalanine ring), 1323 cm^{-1} (C−H bending) are found with the decreased in intensities in the spectrum of the lab-synthesized drug in comparison to tinidazole which might be due to the degradation or disintegration of proteins present in the bacteria.[49] The SERS features at 1237 cm^{-1} (amide III), 1416 (indole rings residue bands of tryptophan), 1450 cm^{-1} (CH2 bending), 1564 cm^{-1} (N−H bending) are observed with increased intensities due to the exposure of the lab-synthesized drug while remained almost same in the spectra of bacterial samples exposed to tinidazole. Moreover, these SERS features are associated with bacterial cell proteins and an increase in their intensities shows the synthesis of stress-related proteins after exposure to the lab-synthesized drug.[50] The SERS features at 849 cm^{-1} (C−O−C stretching in 1,4-glycosidic link) and 1109 cm^{-1} (C−C asymmetric ring breathing of carbohydrates) are increased by applying the lab drug which may be due to an increase in the amount of pentose phosphate pathways (PPP) intermediates.[22] A decrease in the SERS

https://doi.org/10.1021/acsomega.3c08196
ACS Omega 2024, 9, 6861−6872

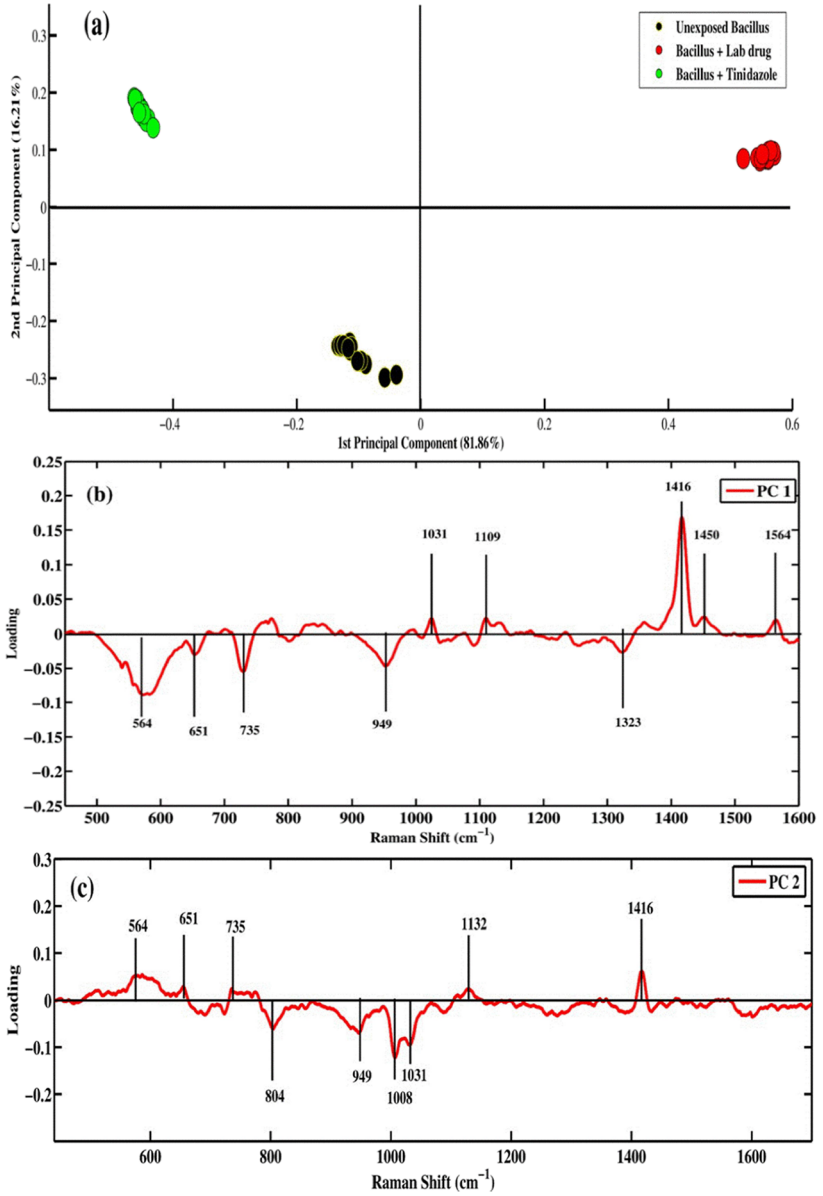

Figure 2. (a) PCA scatter plot of SERS spectral data sets of three samples including untreated and treated *Bacillus subtilis* with tinidazole and lab drug. (b) PCA loadings of PC-1. (c) PCA loadings of PC-2.

intensity at 1031 cm^{-1} (C−O−C stretching band of glycosidic) is seen in the SERS spectrum of bacteria under the exposure of the lab drug and commercial drug tinidazole and a decrease in the intensity leads to a decrease in the concentration of carbohydrates.[51]

A significant enhancement in the intensity of the SERS band observed at 1132 cm^{-1} (unsaturated fatty acid) in bacteria due to exposure to the lab-synthesized drug shows an increase in the degree of saturation of unsaturated fatty acids,[52] while remaining unchanged in the spectra of tinidazole exposed bacteria. It is important to mention that exposure to the lab-synthesized drug is found to cause different biochemical changes in the SERS spectrum of treated bacteria as compared to the spectrum of bacterial samples of the commercially available drug tinidazole, which causes changes only related to increase or decrease of intensities in the SERS features of the bacteria.

2.1. Principal Component Analysis (PCA). As shown in Figure 2a, the PCA scatter plot of the SERS spectral data sets is shown where three distinct clusters, represented by various colors, have been formed by the separation and differentiation of spectra. In each cluster, one dot represents one spectrum where the green cluster assembles along the positive axis of the principal component (PC-1) and shows SERS spectral data sets of bacteria exposed with tinidazole while the black color represents the spectra of the untreated bacillus bacterial samples, and the red cluster on the positive axis represents bacteria treated with the lab drug. Mainly PCA differentiated SERS spectra of unexposed *Bacillus subtilis* from those treated with lab drug and tinidazole.

The maximum source of variation in the data is explained by PC-1, accounting for 81.86% variability, whereas PC-2 describes the remaining variability. PCA is used to find and confirm the characteristic SERS spectral features belonging to the differentiation of three separate spectral data sets of untreated *Bacillus subtilis*, treated *Bacillus subtilis* with tinidazole, and the lab drug in the form of representative PCA loadings which indicate that SERS can examine changes

https://doi.org/10.1021/acsomega.3c08196
ACS Omega 2024, 9, 6861−6872

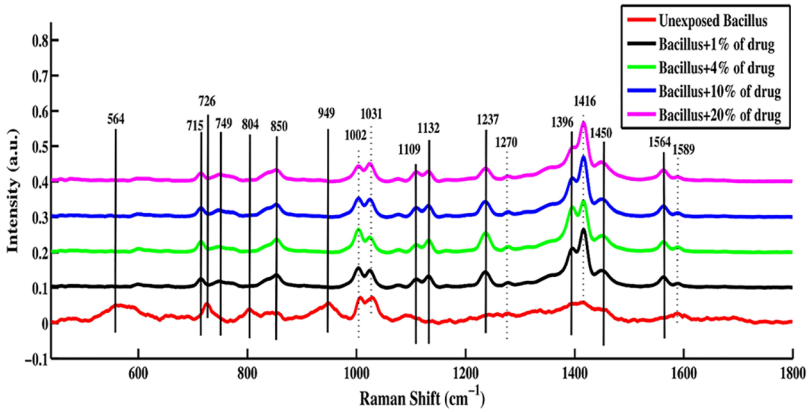

Figure 3. Mean SERS spectra of unexposed *Bacillus subtilis* and exposed *Bacillus subtilis* with different concentrations including 20, 10, 4, and 1% of the lab-synthesized drug.

in the spectral characteristics related with the biochemical alterations induced by various concentrations of the drug synthesized in the lab (Imidazole derivative) in the *Bacillus subtilis* bacteria.

Figure 2b,c shows the PCA loadings of PC-1 and of PC-2, respectively. Figure 2b demonstrates the PCA loadings of data sets of untreated bacillus and treated bacillus with the lab drug which illustrates the separation in the form of negative and positive loadings. These dominant features are observed at 1031, 1109, 1416, 1450, and 1564 cm^{-1} which belong to the positive loadings and characteristics at 564, 651, 735, 949, and 1323 cm^{-1} belong to negative loadings which in turn are related with the SERS spectral data sets of untreated and treated bacillus with in house synthesized drug which is grouped in the negative and positive axis of the PC-1, respectively. The characteristic PCA loadings of Figure 2c including 564, 651, 735, 1132, 1416 cm^{-1}, belong to positive loadings, and 804, 949, 1008, 1031 cm^{-1} which are observed as negative loadings. Notably, these negative and positive loadings are associated with the SERS spectra of unexposed and exposed to commercial drug tinidazole which are grouped in the negative and positive axes of PC-2, respectively. These PCA loadings enable the identification of biochemical changes caused by the commercial drug tinidazole on bacteria and confirm the differentiating characteristics noticed in the mean SERS spectra presented in Figure 1. The PC loadings may be considered as the orthogonal dimensions of variation that allow for the differentiation of various groups in SERS spectral data sets with their coefficients as spectra of each sample scores along these dimensions.

Figure 3 demonstrates the mean SERS spectra of exposed *Bacillus subtilis* with different doses including 1, 4, 10, and 20% of the in-house-synthesized drug and unexposed *Bacillus subtilis*. All the SERS features that are common in all spectra and have intensity-based differences are marked by dotted lines, while SERS features that are not observed in unexposed *Bacillus subtilis* but appear in the bacteria on exposure to different concentrations of the lab drug are marked by solid lines. The SERS bands in the region of 700−800 cm^{-1} associated with DNA features are noticed. The SERS feature at 726 cm^{-1} (adenine/DNA), associated with the bacterial cell, diminished after exposure to the imidazole lab drug. This feature indicates that lab drugs destroyed the bacterial DNA and can be considered as evidence of cell death.[52] Other changes in the SERS bands include 564 cm^{-1} (C−S−S−C), 949 cm^{-1} (single bond stretching vibrations for the amino acids), and diminished on the exposure of lab drug concentrations. Another SERS band decrease in intensity was observed at 1002 cm^{-1} (C−C aromatic ring stretching (phenylalanine) with a gradual increase in the concentration of the lab-synthesized drug which shows that this trend might be due to the degradation or deformation of protein structure in a bacterial cell and cell wall.[52] Other important features assigned for proteins are observed at 715 cm^{-1} (C−N stretching), 1237 cm^{-1} (amide III), 1270 cm^{-1} (amide-III), 1396 cm^{-1} (*N*-acetylglucosamine), 1416 cm^{-1} (tryptophan), 1450 cm^{-1} (CH_2 bending, C−H deformation), 1564 cm^{-1} (N−H bending) in the spectra of *Bacillus subtilis* treated with various doses of the lab drug. Moreover, these SERS features are associated with bacterial cell proteins, and an increase in intensities shows the synthesis of stress-related proteins under the stress caused by exposure to the lab-synthesized drug.[53]

The SERS features observed at 849 cm^{-1} (C−O−C stretching in 1,4-glycosidic link), 1109 cm^{-1} (carbohydrates), and 1031 cm^{-1} (C−O−C stretching band of the glycosidic link) are increased in intensities by applying the lab drug which might be due to increase in the amount of pentose phosphate pathways (PPP) intermediates.[54] Moreover, a significant increase in the intensity of the band observed at 1132 cm^{-1} (unsaturated fatty acid) might be due to an increase in the degree of saturation of unsaturated fatty acids as a result of stress caused in the bacterial cell.[55]

2.2. Principal Component Analysis (PCA). Pairwise PCA is applied to determine which SERS spectral characteristics are involved in differentiating between the SERS spectral data sets in the form of PCA loadings. Figure 4a shows a pairwise PCA scatter plot of the two different SERS spectra data sets of unexposed bacillus and its treatment with 20% of the lab drug, indicating clear differentiation between them, and it can be seen that maximum variability between them is explained by PC-1 which accounts 78.3% variation. As seen in Figure 4a, the negative and positive PCA loadings belong to the SERS spectral data sets grouped on the positive and negative axis of the PC-1, respectively, as represented in the PCA scatter plot in Figure 4a. The well-separated clusters shown in the PCA scatter plot indicate that there are significant biochemical differences between them.

Figure 4b represents the PCA loadings plot of PC1 of Figure 4a that illustrates the significant features that are changed due to the biochemical alterations in the bacterial cell caused by the

https://doi.org/10.1021/acsomega.3c08196
ACS Omega 2024, 9, 6861−6872

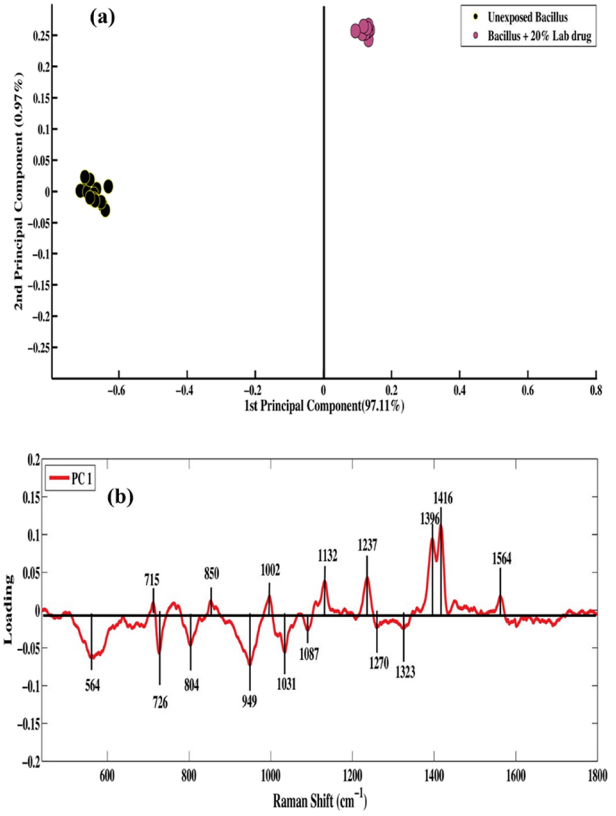

Figure 4. (a) PCA scatter plot of SERS spectral data sets of exposed *Bacillus subtilis* with 20% of the lab-synthesized drug and unexposed *Bacillus subtilis*. (b) PCA loadings of PC-1.

exposure of the lab-synthesized drug. The PCA loadings of SERS spectral data sets of untreated and treated bacillus with 20% drug are shown in Figure 4b, which reflects the cause of differentiation of features in the positive and negative loadings. These dominant features in Figure 4b at 715, 850, 1002, 1132, 1237, 1396, 1416, and 1564 cm^{-1} belonging to positive loadings of *Bacillus subtilis* exposed with the lab-synthesized drug. Other characteristic SERS features include 564, 726, 804, 949, 1031, 1087, 1270, and 1323 cm^{-1} which are observed as negative loadings. These PCA loadings enable the identification of biochemical changes caused by lab-synthesized drugs on bacteria and confirm the differentiating features observed in the mean SERS spectra presented in Figure 3. The PC loadings may be considered as the orthogonal dimensions of variability that allow for the differentiation of various groups in SERS spectral data sets along their coefficients, as spectra of each sample score along these dimensions.

2.3. Partial Least-Squares Discriminant Analysis (PLS-DA). PLS-DA is a supervised approach that can be used for discriminative variable selection as well as for descriptive and predictive modeling. This model was applied for the quantitative discrimination between untreated and treated bacillus with different concentrations of the lab drug derivative by utilizing the previous information on classes. By incorporating class information, PLS-DA helps differentiate various groups, such as untreated and treated *Bacillus subtilis*, and it identifies latent variables that enable distinct separation of relevant SERS spectra. This results in a more reliable classification compared to PCA alone.

To prevent overtraining, the SERS spectral data sets were randomized and then split into two sets: a training data set (60% spectra) and a test data set (40% spectra). Montecarlo cross-validation based on the Bayes theorem was employed for PLS-DA. The variables with the least error were identified in order to select optimal latent variables (OptLVs) with high accuracy. Ten optimal latent variables were recognized through cross-validation, and the PLS-DA model was trained with the calibration data set. The performance of the model was assessed by the trained model because the validation data set was different from the training data set.

To assess the model's performance, the trained discrimination model was employed to the test data set using OptLVs that are shown in Figure 5a which shows that SERS spectral data sets of various doses of the lab-synthesized drug are clearly differentiated by PLS-DA model.

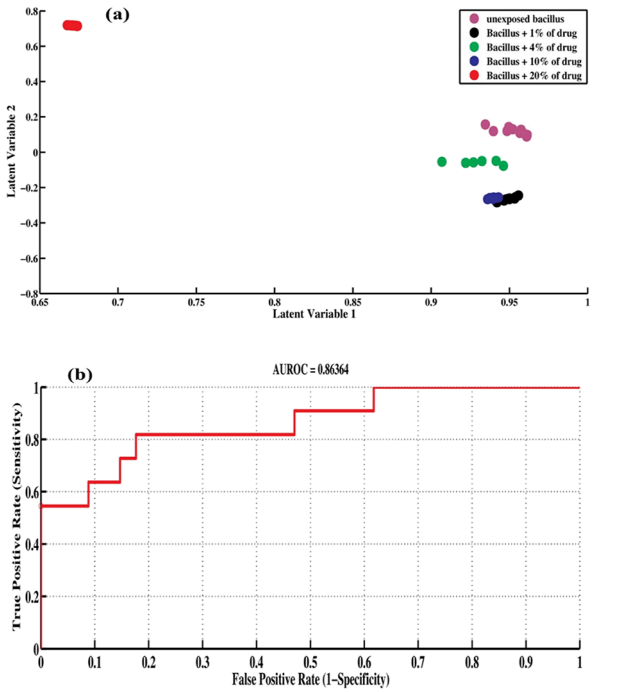

Figure 5. (a) Score plot of PLS-DA for the validation of SERS spectral data set of unexposed *Bacillus subtilis* and its exposure with four different concentrations of lab-synthesized drug. (b) Receiver operating characteristic (ROC) curve for the performance of the PLS-DA discrimination model for SERS spectral data sets of unexposed and exposed *Bacillus subtilis*.

The PLS-DA model is employed to evaluate the efficacy of the discrimination of different groups of SERS spectral data sets, as done by PCA, and the identification and differentiation potential of the SERS technique. For this purpose, the receiver operating characteristic (ROC) curve can be a reliable approach, as shown in Figure 5b. The ROC curve between the true positive rate (sensitivity) and the false-positive rate (1 specificity) has been plotted. The maximum value of AUC is 1, which demonstrates that a model with a value closer to 0 does not perform well or perform poorly, while a model with a value closer to 1 is more reliable and ideal. The area covered under the ROC curve was 0.86, showing that the model performed well because it is closer to 1.

2.4. Partial Least-Squares Regression (PLSR) Analysis. PLSR is used for quantitative analysis which allows the prediction of different concentrations of in-house-synthesized drugs. The optimal number of latent variables is 10 providing

https://doi.org/10.1021/acsomega.3c08196
ACS Omega 2024, 9, 6861−6872

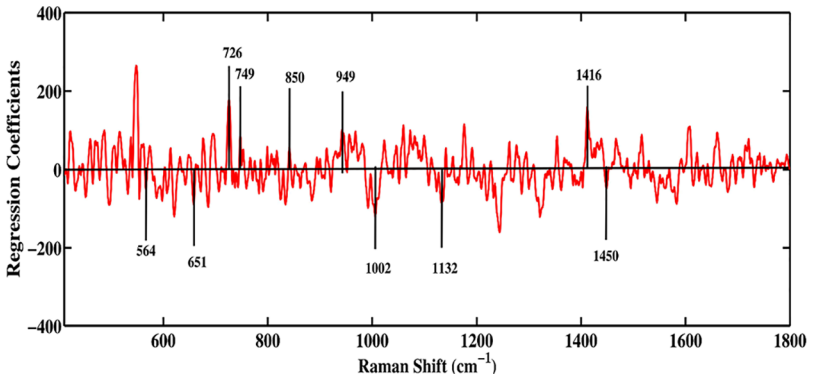

Figure 6. Regression coefficient for spectral data of different concentrations of the lab-synthesized drug.

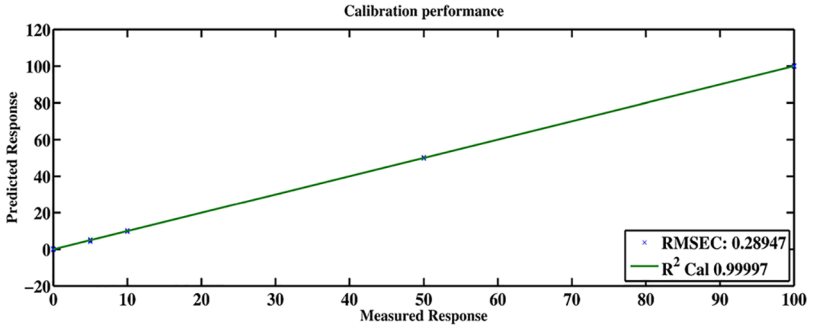

Figure 7. Performance of the PLSR model with calibration and prediction for Raman spectral data.

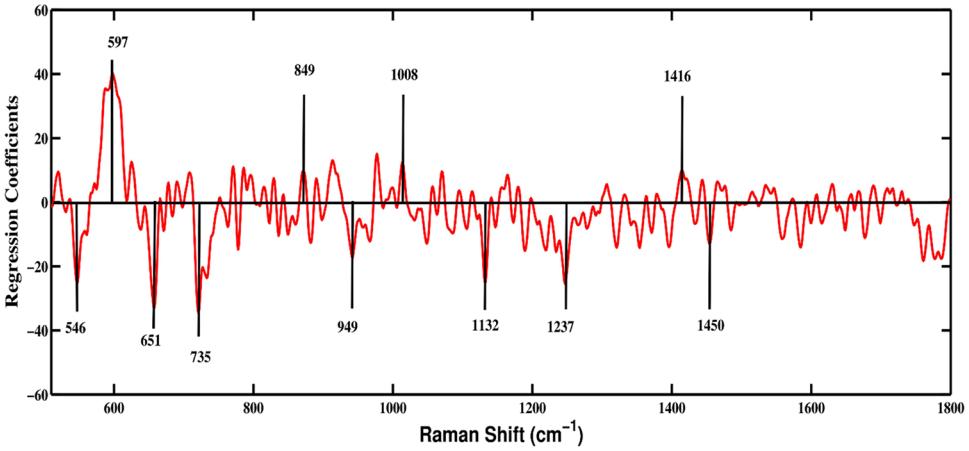

Figure 8. Regression coefficient for spectral data of commercially available drug tinidazole.

RMSECV is 0.29, and the R^2 value of goodness of the model is found to be 0.99 (Figure 7).

2.5. Regression Coefficients. The regression coefficient obtained from PLSR analysis is shown in Figure 6. The features at 726, 749, 850, 949, 1416, 564, 651, 1002, 1132, and 1450 cm^{-1} have been discussed in detail earlier. These specific dominant features are noticed successfully in both mean SERS spectra and PLSR analysis (Figure 7). These characteristics enable the identification of biochemical changes caused by lab-synthesized drug formulations on bacteria and verify the differentiating features observed in mean SERS spectra presented in Figure 3.

The regression coefficient obtained from PLSR analysis for commercially available drug tinidazole is shown in Figure 8, features at 546, 597, 651, 849, 949, 1008, 1132, 1237, 1416, and 1450 cm^{-1}. These dominant features ensure the antibacterial activity of tinidazole on the bacillus and have been discussed in detail earlier. These specific dominant features are properly identified in both mean SERS spectra and PLSR analysis as well. These features enable the identification of biochemical changes caused by commercially available tinidazole drug formulations on bacteria and ensure the differentiating features observed in mean SERS spectra presented in Figure 1.

"PLSR is employed for quantitative analysis which makes it practicable to estimate various concentrations of imidazole. An optimal number of latent variables is 10 providing an RMSECV value of 3.4269, and the R^2 value of goodness of the model is found to be 0.9893 (Figure 9)."

https://doi.org/10.1021/acsomega.3c08196
ACS Omega 2024, 9, 6861−6872

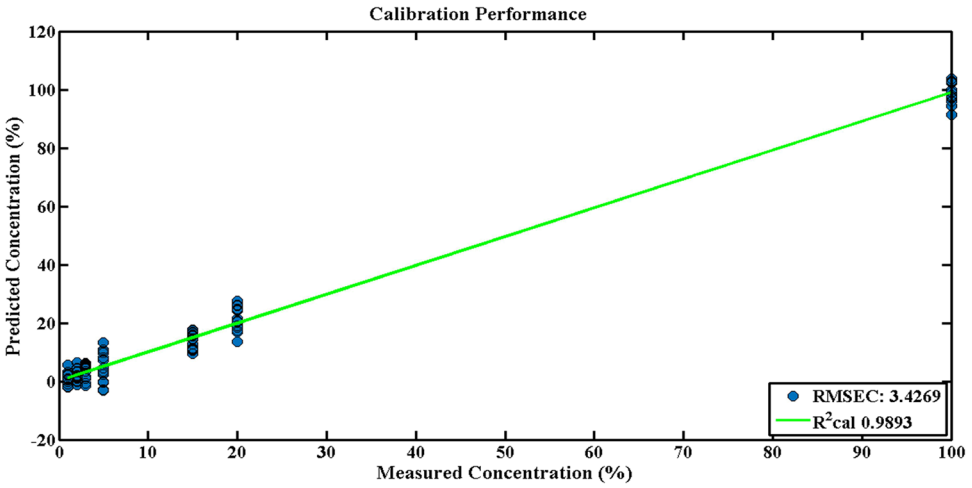

Figure 9. Performance of PLSR on five data sets including unexposed bacillus and exposed with various concentrations 1, 4, 10, and 20% of commercially available drug tinidazole.

3. MATERIALS AND METHODS

3.1. Synthesis of Bromide Salt of Imidazole. Imidazole (2.0 g, 29.3 mmol), dimethyl sulfoxide (30 mL), and 1.5 equiv KOH (2.47 g, 44 mmol) were placed in a round-bottom flask and stirred in a water-containing beaker for 30 min. One equivalent of 1-bromo-3-methylbutane (4.43 g, 29.3 mmol) was added dropwise, as the reaction is exothermic, so cool water was added to a stirring beaker to maintain the reaction media's temperature. *N*-Alkylated compound (1-isopentyl-1*H*-imidazole) having a yield of 92.30% was synthesized. In the next step, in a round-bottom flask, an *N*-alkylated compound (2.0 g, 14.4 mmol) was taken and dissolved in 1,4-dioxane (30 mL). While being constantly stirred, 1-bromopentane (2.18 g, 13.24 mmol) was added drop by drop in the solution. At 100 °C, the reaction mixture was refluxed for 22 h. *N*-Hexane was used twice to wash the product solution; an oily, brownish product was obtained. Yield: 86.53%.

3.1.1. FT-IR Characterization. Synthesis of imidazolium salt (1-isopentyl-3-pentyl-2,3-dihydro-1*H*-imidazole, bromide salt) was completed in two separate phases according to the protocol of.[56] *N*-Alkylation of imidazole was initially accomplished via a simple reaction of alkyl imidazole in basic media. The following stage produces imidazolium salt by alkylating imidazole at its second nitrogen (N2) by reflux in 1,4-dioxane, as elaborated in Scheme 1. The yield product was

Scheme 1. Synthesis of *N*-Alkylated Compound in Step-I and Salt in Step-II

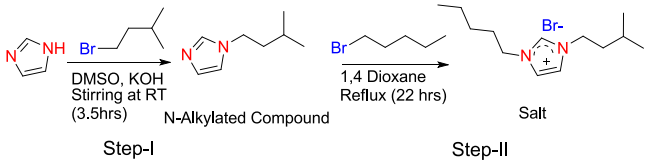

oily in nature having a brownish color and had higher density in the reaction mixture due to which it was allowed to settle at the bottom of the flask. The reaction mixture was decanted carefully, and then, the last salt was washed with *n*-hexane. The resulting mixture is soluble in chloroform, and to purify it, this solution is run through Celite. The resulting product is subjected to a check purification through TLC.

In the experimental FT-IR spectra, very short-ranged peaks (3500−500 cm^{-1}) were noticed. Higher and lower frequency of C−H stretching is seen below 3000 cm^{-1} as a result of symmetric and antisymmetric C−H stretching. Between 1200 and 1800 cm^{-1}, stretching vibrations of C−C were observed, and below 500 cm^{-1}, C−C bending vibrations were found. Bending vibrations of CH3 and CH2 were found at 1162.9 and 1369.8 cm^{-1}, respectively. FT-IR (ATR cm^{-1}): 2963.2,2870.0 (C−H str), 1636.3,1552.4 (C═C str), 1559.9, 1459.3 (C−C str), 1217.0,1183.4 (C−N str), 760.4,680.2 (C- H bend).[57]

3.2. NMR Characterization. NMR characterization is performed for the confirmation of the synthesis of imidazole salt. The acidic proton of the carbene carbon's resonance frequency was found around 8−10 ppm, which is one of the distinctive properties found in the ^{1}H NMR spectra obtained during ligand analysis. This resonance frequency appeared as a carbene proton significant feature and was detected at 9.24 ppm. A related pattern has also been observed in the literature, demonstrating how *N*-heterocyclic carbene compounds are distinctively correlated with the appearance of the resonance frequency of the carbene proton.[57] ^{13}C NMR spectroscopy provided similar substantial proof of the effective synthesis of the designed salt. For synthesized salt, the resonance frequency of carbene carbon was found to be prominently featured, in a range of 135.92 ppm.

3.3. Bacterial Culture. The antibacterial potential of the in-house-synthesized salt (1-isopentyl-3-pentyl-1*H*-imidazole-3-ium bromide salt), submitted elsewhere, and tinidazole named Fasigyn was evaluated for Gram-positive bacteria (Scheme 2). The concentration of these bacteria was maintained at 108 cells/ml for the duration of a night incubation period in a rotary shaker with Mueller Hinton broth (MHB) at 37 °C.

3.4. Bioassay for the Determination of Antibacterial Activity. The antibacterial efficiencies of different doses of lab-synthesized salt (1-isopentyl-3-pentyl-1*H*-imidazole-3-ium bromide salt) and tinidazole were tested using the agar well diffusion technique against *Bacillus subtilis*. For this purpose, in a sterile Petri dish, 1 mL of freshly cultured bacteria was added to the center along with cooled and melted Mueller Hinton broth containing the inoculum, and everything was mixed thoroughly. Following the solidification of the broth, the inoculum wells were filled with 100 mL of lab-synthesized salt

https://doi.org/10.1021/acsomega.3c08196
ACS Omega 2024, 9, 6861−6872

Scheme 2. Imidazolium Bromide (1-Isopentyl-3-pentyl-1*H*-imidazole-3-ium Bromide Salt), Chemical Formula: $C_{13}H_{25}BrN_2^-$, Molecular Weight: 289.26

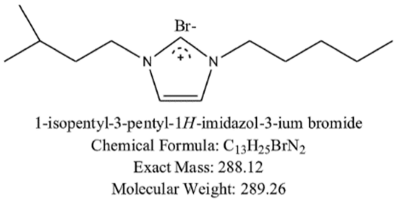

in varying concentrations including 1, 4, 10, and 20%). After 18 h at 37 °C, these plates were incubated to determine the antibacterial activity of various doses against *Bacillus subtilis*, a Gram-positive bacterial strain. To analyze the antibacterial potency of various doses of in-house-synthesized salt and tinidazole, the breadth of the wells as well as the zone of inhibition was determined (Figure 10a,b).

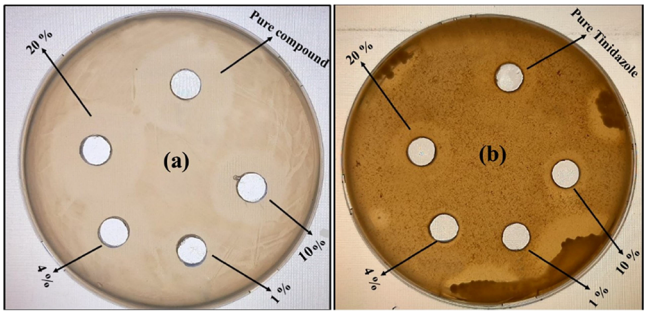

Figure 10. (a) Zone of inhibition test for assessing the antibacterial efficacy of an imidazole derivative (1-isopentyl-3-pentyl-1*H*-imidazole-3-ium bromide salt) produced in the lab and (b) commercial drug tinidazole against *Bacillus subtilis*.

Figure 10a,b shows the disk-diffusion method for testing the biological activity of in-house-produced drugs and commercially available drugs against bacteria (*Bacillus subtilis*) respectively. Figure 10a,b shows five zones of inhibition. Notably, as commercially available tinidazole and the concentrations of the in-house-synthesized salt increased, the zone of inhibition increased. It is clearly observed from the results of the bioactivity assay (Table 1) that zones of inhibition values for different doses (1, 4, 10, 20%, and pure compound) of the lab drug are greater in contrast to tinidazole. Notably, the efficacy of the lab-synthesized drug dominates the marketed drug. Furthermore, this is explained in the mean SERS spectra of in-house-synthesized drug and tinidazole Figure 11. The bioactivity assay results validate the SERS findings. Table 2 provides an overview of the results of the bioactivity experiment.

Table 2. Zones for Inhibition Determination

pharmaceutical concentrations (%)	inhibition zone (mm) lab drug	inhibition zone (mm) tinidazole
1	14	0
4	20	4
10	28	10
20	35	11
pure compound	41	16

The mean SERS spectra of in-house-synthesized drug (1-isopentyl-3-pentyl-1*H*-imidazole-3-ium bromide salt) and commercially available pharmaceutical drug tinidazole are shown in Figure 11. It is clear that there is no feature of Figure 1 derived from the drugs themselves. All the features explained in Figure 1 are related to antibacterial activity.

Lab-synthesized drug and tinidazole have shown spectral features at 437, 485, 617, 656, 832, 991, 1124, 1185, 1263, 1349, 1365, 1375, 1414, 1480, 1485 cm^{-1} in mean Raman spectra, which shows that drug features did not appear in Figure 1 during antibacterial activity.

3.5. Preparation of Silver Nanoparticles. In this study, silver nanoparticles were synthesized using the chemical reduction process. For this purpose, silver nitrate and trisodium citrate were used as precursors. Trisodium citrate is a capping agent as well as a reducing agent. A solution of silver nitrate (0.0085 g/300 mL) in distilled water was heated to 100 °C before being mixed with 10 mL of 1% trisodium citrate. This solution was boiled with magnetic stirring for 30 min on a hot plate. This resulted in the gray-colored nanoparticles. The silver nanoparticles were characterized by using SEM and TEM with a field emission electron microscope. Preparing TEM samples involves evaporating a silver nanoparticle solution onto a carbon-coated copper grid. A dried drop of silver nanoparticles was placed on a cupric stub with no additional conductive coating for SEM.

According to the electromagnetic mechanism, the nanoparticles with a strong absorption at the excitation wavelength

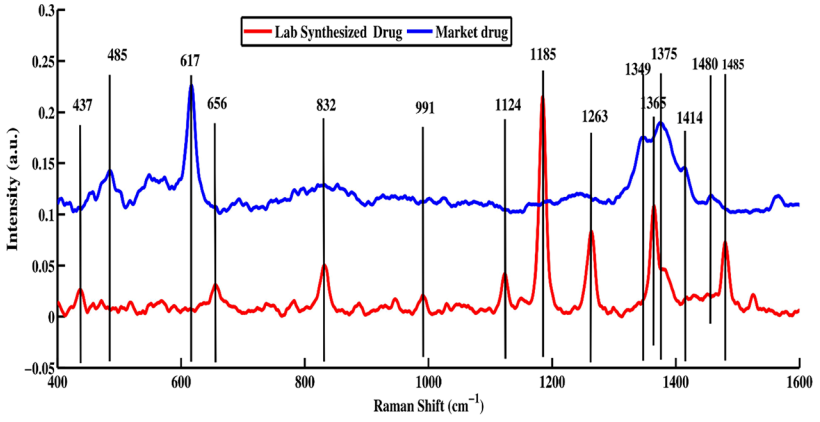

Figure 11. Mean spectra of lab (in house) synthesized drug and pharmaceutical drug tinidazole.

https://doi.org/10.1021/acsomega.3c08196
ACS Omega 2024, 9, 6861−6872

will give a strong resonance enhancement effect than those having small absorption.[29]

3.6. SERS Spectral Acquisition. Surface-enhanced Raman spectra were acquired with a Raman spectrometer (Peak Seeker Pro 785; Agiltron, USA) equipped with a charged coupled detector (CCD). This Raman spectrometer is integrated with a microscope used to view the sample on the substrate. As an excitation source, a diode laser with a monochromatic wavelength of 785 nm was used. The sample of unexposed bacterial pellets (*Bacillus subtilis*) and exposed bacteria with different doses of in-house-synthesized drugs including 1, 4, 10, and 20% and commercial drug tinidazole, 50 μL each, were placed in an Eppendorf tube and incubated for 30 min with 50 μL of silver nanoparticles. After incubation time, on an aluminum slide, a 50 μL sample from the incubation mixture was taken and 15 Raman spectra were acquired for every sample by focusing the laser on the sample. With the laser power of 50 mW and 10 s spectral acquisition time, a 40X objective lens was utilized.

3.7. Data Preprocessing Algorithms. To convert raw SERS spectral data into useful informative spectral data, preprocessing algorithms were required for removing interfering factors. All the fundamental preprocessing algorithms, including vector normalization (VN), substrate removal, baseline correction, and smoothing were done using MATLAB R2009a (The MathWorks, USA) and its standard chemometric models using in-house-built codes. The background/substrate (aluminum slide) elimination was done by using a subtraction approach from SERS spectral data followed by its vector normalization, and the Savitzky−Golay algorithm was used for smoothing of spectral data with a 13-point window width.

4. MULTIVARIATE DATA ANALYSIS

For the analysis of SERS spectral data sets, mean SERS spectra were obtained for every bacterial sample including bacillus unexposed and bacillus treated with a lab drug and tinidazole. The SERS spectral characteristics utilized in the interpretation of the SERS bands were found in the literature and are listed in Table 1 with the citations of the references for each band assignment. For more evaluation of a multivariate data set, several chemo-metric analytical approaches were utilized to increase the variance across spectral signatures such as PCA and PLS-DA, which were employed to examine the preprocessed data of Bacillus strains across the whole spectral range between 400 and 1800 cm^{-1}.

PCA is an unsupervised approach for analyzing spectral data sets and determining the dominant patterns of variability in the matrix of spectra of different samples. PCA converts the correlated variables into uncorrelated variables, which are called PC scores, which maintain the variability in the spectral data while eliminating random (noise) variation. Most of the variation in the spectral data is explained by the first PC and the remaining variability is explained by the next PC.[58] Although PCA is well adapted to highlight the presence of clusters in the data set, other less significant biological parameters, such as spectral features not associated with a pathological condition, may have an impact on the data distribution over the scatter plot. Consequently, it seems that in order to achieve discrimination, a supervised constraint on the PCA was added to give underlying spectral information more weight in the classification.[59]

In MATLAB R2009a (The MathWorks, USA), PLS-DA was applied to enhance and improve the diagnostic potential of SERS which provides more accurate discrimination. It takes advantage of prior class information to provide a more robust discrimination between SERS spectral data of bacillus treated with various concentrations of imidazole derivative and unexposed ones. The class information was used as the y-variables and the SERS spectral data was used as the *x*-variables in the PLS-DA. In PLS-DA, binary discrimination was employed in the current work to categorize the spectral data of bacterial strain while cross-validation was used to find out the optimal number of latent variables (LVs).[60]

PCA and PLS-DA were used to differentiate and discriminate the effects of different dosages of antibiotic treatments on Bacillus bacteria. In this study, PLS-DA was used for discrimination among SERS spectral data sets to analyze the biochemical alterations induced in bacteria by exposure to antibiotics.

5. CONCLUSIONS

This work shows that SERS coupled with multivariate data analysis techniques such as PCA and PLS-DA can distinguish among unexposed *Bacillus subtilis* and its treatment with in-house-synthesized drug and commercial drug tinidazole. SERS has identified various biochemical changes in the form of SERS spectral features at 546, 715, 850, 1002, 1132, 1270, 1396, 1416, and 1453 cm^{-1}, which have been found in the literature reported for their association with antibacterial activity. This shows that SERS in combination with multivariate data analysis techniques, including PCA and PLS-DA, and PLSR analysis can successfully be used to analyze the antibacterial activity of potential by newly synthesized antibacterial drug candidates.

■ ASSOCIATED CONTENT

Supporting Information

The Supporting Information is available free of charge at https://pubs.acs.org/doi/10.1021/acsomega.3c08196.

Mean SERS spectra of exposed and unexposed *Bacillus subtilis* with different concentrations of lab-synthesized drug and tinidazole (PDF)

■ AUTHOR INFORMATION

Corresponding Authors

Muhammad Irfan Majeed − *Department of Chemistry, University of Agriculture Faisalabad, Faisalabad 38000, Pakistan;* orcid.org/0000-0003-0506-6060; Email: irfan.majeed@uaf.edu.pk

Abeer Ahmed Alghamdi − *Department of Physics, College of Science, Princess Nourah bint Abdulrahman University, Riyadh 11671, Saudi Arabia*; Email: abaalghamdi@pnu.edu.sa

Haq Nawaz − *Department of Chemistry, University of Agriculture Faisalabad, Faisalabad 38000, Pakistan;* orcid.org/0000-0003-2739-4735; Email: haqchemist@yahoo.com

Authors

Fatima Tahir − *Department of Chemistry, University of Agriculture Faisalabad, Faisalabad 38000, Pakistan*

Ali Kamran − *Department of Chemistry, University of Agriculture Faisalabad, Faisalabad 38000, Pakistan*

https://doi.org/10.1021/acsomega.3c08196
ACS Omega 2024, 9, 6861−6872

Muhammad Rizwan Javed − *Department of Bioinformatics and Biotechnology, Government College University Faisalabad (GCUF), Faisalabad 38000, Pakistan*
Muhammad Adnan Iqbal − *Department of Chemistry, University of Agriculture Faisalabad, Faisalabad 38000, Pakistan*; orcid.org/0000-0001-6241-7547
Muhammad Tahir − *Department of Chemistry, University of Agriculture Faisalabad, Faisalabad 38000, Pakistan*
Anam Tariq − *Department of Biochemistry, Government College University Faisalabad (GCUF), Faisalabad 38000, Pakistan*
Nosheen Rashid − *Department of Chemistry, University of Education, Faisalabad Campus, Faisalabad 38000, Pakistan*
Urwa Shahid − *Department of Chemistry, University of Agriculture Faisalabad, Faisalabad 38000, Pakistan*
Ahmad Hassan − *Department of Chemistry, University of Agriculture Faisalabad, Faisalabad 38000, Pakistan*
Umar Sohail Shoukat − *Department of Chemistry, University of Agriculture Faisalabad, Faisalabad 38000, Pakistan*

Complete contact information is available at: https://pubs.acs.org/10.1021/acsomega.3c08196

Author Contributions

#F.T. and A.K. equally contributed to this work.

Notes

The authors declare no competing financial interest.

■ ACKNOWLEDGMENTS

The authors express their gratitude to Princess Nourah bint Abdulrahman University Researchers Supporting Project number (PNURSP2024R451), Princess Nourah bint Abdulrahman University, Riyadh, Saudi Arabia.

■ REFERENCES

(1) Sprigg, K.; Pietrangeli, C. E. Bacterial antibiotic resistance: on the Cusp of a post-antibiotic world. *Current Treatment Options in Infectious Diseases* **2019**, *11*, 42−57.
(2) Petchiappan, A.; Chatterji, D. Antibiotic resistance: current perspectives. *ACS omega* **2017**, *2* (10), 7400−7409.
(3) Wang, P.; Wang, X.; Sun, Y.; Gong, G.; Fan, M.; He, L. Rapid identification and quantification of the antibiotic susceptibility of lactic acid bacteria using surface enhanced Raman spectroscopy. *Analytical Methods* **2020**, *12* (3), 376−382.
(4) Reller, L. B.; Weinstein, M.; Jorgensen, J. H.; Ferraro, M. J. Antimicrobial susceptibility testing: a review of general principles and contemporary practices. *Clin. Infect. Dis.* **2009**, *49* (11), 1749−1755.
(5) Aher, S.; Das, A.; Muskawar, P.; Osborne, J.; Bhagat, P. Synthesis, characterization and antimicrobial properties of methylbenzyl and nitrobenzyl containing imidazolium-based silver N-heterocyclic carbenes. *J. Mol. Liq.* **2017**, *233*, 270−277.
(6) Talib, M. K.; Ghadhyeb, M. Z. Antibacterial activity, synthesis and characterization of a new Ag (I) and Pd (II) complexes with N-heterocyclic carbene. *J. Kufa Chem. Sci.* **2023**, *2* (10), 11877.
(7) Ronga, L.; Varcamonti, M.; Tesauro, D. Structure−Activity Relationships in NHC−Silver Complexes as Antimicrobial Agents. *Molecules* **2023**, *28* (11), 4435.
(8) Rani, N.; Sharma, A.; Singh, R. Imidazoles as promising scaffolds for antibacterial activity: a review. *Mini reviews in medicinal chemistry* **2013**, *13* (12), 1812−1835.
(9) Duan, Y.-T.; Wang, Z.-C.; Sang, Y.-L.; Tao, X.-X.; Zhu, H.-L. Exploration of structure-based on imidazole core as antibacterial agents. *Current topics in medicinal chemistry* **2013**, *13* (24), 3118−3130.
(10) Chen, L.; Zhao, B.; Fan, Z.; Liu, X.; Wu, Q.; Li, H.; Wang, H. Synthesis of novel 3, 4-chloroisothiazole-based imidazoles as fungicides and evaluation of their mode of action. *Journal of agricultural and food chemistry* **2018**, *66* (28), 7319−7327.
(11) Hu, Y.; Shen, Y.; Wu, X.; Tu, X.; Wang, G.-X. Synthesis and biological evaluation of coumarin derivatives containing imidazole skeleton as potential antibacterial agents. *European journal of medicinal chemistry* **2018**, *143*, 958−969.
(12) Rossi, R.; Ciofalo, M. An updated review on the synthesis and antibacterial activity of molecular hybrids and conjugates bearing imidazole moiety. *Molecules* **2020**, *25* (21), 5133.
(13) Khabnadideh, S.; Rezaei, Z.; Khalafi-Nezhad, A.; Bahrinajafi, R.; Mohamadi, R.; Farrokhroz, A. Synthesis of N-alkylated derivatives of imidazole as antibacterial agents. *Bioorg. Med. Chem. Lett.* **2003**, *13* (17), 2863−2865.
(14) Uchida, K.; Nishiyama, Y.; Yamaguchi, H. In vitro antifungal activity of luliconazole (NND-502), a novel imidazole antifungal agent. *Journal of infection and chemotherapy* **2004**, *10* (4), 216−219.
(15) Soraya, S.; Soraya, S. S. Affectivity of the imidazole anticancer drug on the diagnosis of the cancers by using quantum chemical methods. *IPCBEE* **2012**, *29*, 187−190.
(16) Pantala, R.; Khagga, M.; Bhavani, R.; Bhavani, V. Novel Salt of Tinidazole with Improved Solubility and Antibacterial Activity. *Orient. J. Chem.* **2017**, *33* (1), 490−499.
(17) Saleem, M.; Majeed, M. I.; Nawaz, H.; Iqbal, M. A.; Hassan, A.; Rashid, N.; Tahir, M.; Raza, A.; Ul Hassan, H. M.; Sabir, A. Surface-Enhanced Raman Spectroscopy for the Characterization of the Antibacterial Properties of Imidazole Derivatives against Bacillus subtilis with Principal Component Analysis and Partial Least Squares−Discriminant Analysis. *Anal. Lett.* **2022**, *55*, 2132−2146.
(18) Turnbull, P. C.; Kramer, J.; Melling, J. Bacillus *Med. Microbiol.* **1996**, *4*.
(19) Gindri, I. M.; Siddiqui, D. A.; Bhardwaj, P.; Rodriguez, L. C.; Palmer, K. L.; Frizzo, C. P.; Martins, M. A.; Rodrigues, D. C. Dicationic imidazolium-based ionic liquids: A new strategy for non-toxic and antimicrobial materials. *RSC Adv.* **2014**, *4* (107), 62594−62602.
(20) Pałkowski, Ł.; Błaszczyński, J.; Skrzypczak, A.; Błaszczak, J.; Kozakowska, K.; Wróblewska, J.; Kożuszko, S.; Gospodarek, E.; Krysiński, J.; Słowiński, R. Antimicrobial Activity and SAR Study of New Gemini Imidazolium-Based Chlorides. *Chemical Biology & Drug Design* **2014**, *83* (3), 278−288.
(21) Molvi, K.; Sudarsanam, V.; Haque, N. Synthesis and Antibacterial Activity of Some 2-Substituted Tinidazole Analogues. *Ethiopian Pharma. J.* **2007**, *25* (1), 43−50.
(22) Voloshina, A. D.; Gumerova, S. K.; Sapunova, A. S.; Kulik, N. V.; Mirgorodskaya, A. B.; Kotenko, A. A.; Prokopyeva, T. M.; Mikhailov, V. A.; Zakharova, L. Y.; Sinyashin, O. G. The structure−activity correlation in the family of dicationic imidazolium surfactants: Antimicrobial properties and cytotoxic effect. *Biochimica et Biophysica Acta (BBA)-General Subjects* **2020**, *1864* (12), No. 129728.
(23) Wang, L.; Qin, H.; Ding, L.; Huo, S.; Deng, Q.; Zhao, B.; Meng, L.; Yan, T. Preparation of a novel class of cationic gemini imidazolium surfactants containing amide groups as the spacer: Their surface properties and antimicrobial activity. *J. Surfactants Deterg.* **2014**, *17*, 1099−1106.
(24) Alou, L.; Giménez, M.; Manso, F.; Sevillano, D.; Torrico, M.; González, N.; Granizo, J.; Bascones, A.; Prieto, J.; Maestre, J. Tinidazole inhibitory and cidal activity against anaerobic periodontal pathogens. *Int. J. Antimicrob. Agents* **2009**, *33* (5), 449−452.
(25) Zhang, B.; Cui, L.; Zhang, K. Dosage-and time-dependent antibacterial effect of zinc oxide nanoparticles determined by a highly uniform SERS negating undesired spectral variation. *Anal. Bioanal. Chem.* **2016**, *408* (14), 3853−3865.
(26) Jarvis, R. M.; Goodacre, R. Characterisation and identification of bacteria using SERS. *Chem. Soc. Rev.* **2008**, *37* (5), 931−936.
(27) Jarvis, R. M.; Goodacre, R. Discrimination of bacteria using surface-enhanced Raman spectroscopy. *Analytical chemistry* **2004**, *76* (1), 40−47.
(28) Zhang, Z.; Han, X.; Wang, Z.; Yang, Z.; Zhang, W.; Li, J.; Yang, H.; Ling, X. Y.; Xing, B. A live bacteria SERS platform for the in situ

monitoring of nitric oxide release from a single MRSA. *Chem. Commun.* **2018**, *54* (51), 7022−7025.
(29) Zeng, J.; Jia, H.; An, J.; Han, X.; Xu, W.; Zhao, B.; Ozaki, Y. Preparation and SERS study of triangular silver nanoparticle self-assembled films. *Journal of Raman Spectroscopy: An International Journal for Original Work in all Aspects of Raman Spectroscopy, Including Higher Order Processes, and also Brillouin and Rayleigh Scattering* **2008**, *39* (11), 1673−1678.
(30) Hadjigeorgiou, K.; Kastanos, E.; Pitris, C. Optical Diagnostics and Sensing XIII: Toward Point-of-Care Diagnostics. In *Urinary tract infection (UTI) multi-bacteria multi-antibiotic testing using surface enhanced Raman spectroscopy (SERS)*; SPIE: 2013; pp. 53−59.
(31) Liu, C.-Y.; Han, Y.-Y.; Shih, P.-H.; Lian, W.-N.; Wang, H.-H.; Lin, C.-H.; Hsueh, P.-R.; Wang, J.-K.; Wang, Y.-L. Rapid bacterial antibiotic susceptibility test based on simple surface-enhanced Raman spectroscopic biomarkers. *Sci. Rep.* **2016**, *6* (1), 23375.
(32) Novelli-Rousseau, A.; Espagnon, I.; Filiputti, D.; Gal, O.; Douet, A.; Mallard, F.; Josso, Q. Culture-free antibiotic-susceptibility determination from single-bacterium Raman spectra. *Sci. Rep.* **2018**, *8* (1), 3957.
(33) Reardon-Robinson, M. E.; Ton-That, H. Disulfide-bond-forming pathways in Gram-positive bacteria. *J. Bacteriol.* **2016**, *198* (5), 746−754.
(34) Kashif, M.; Majeed, M. I.; Nawaz, H.; Rashid, N.; Abubakar, M.; Ahmad, S.; Ali, S.; Hyat, H.; Bashir, S.; Batool, F. Surface-enhanced Raman spectroscopy for identification of food processing bacteria. *Spectrochim. Acta A* **2021**, *261*, No. 119989.
(35) Paret, M. L.; Sharma, S. K.; Green, L. M.; Alvarez, A. M. Biochemical characterization of Gram-positive and Gram-negative plant-associated bacteria with micro-Raman spectroscopy. *Applied spectroscopy* **2010**, *64* (4), 433−441.
(36) Premasiri, W.; Moir, D.; Klempner, M.; Krieger, N.; Jones, G.; Ziegler, L. Characterization of the surface enhanced Raman Scattering (SERS) of bacteria. *J. Phys. Chem. B* **2005**, *109* (1), 312−320.
(37) Fan, C.; Hu, Z.; Mustapha, A.; Lin, M. Rapid detection of food- and waterborne bacteria using surface-enhanced Raman spectroscopy coupled with silver nanosubstrates. *Applied microbiology and biotechnology* **2011**, *92*, 1053−1061.
(38) Ciloglu, F. U.; Saridag, A. M.; Kilic, I. H.; Tokmakci, M.; Kahraman, M.; Aydin, O. Identification of methicillin-resistant Staphylococcus aureus bacteria using surface-enhanced Raman spectroscopy and machine learning techniques. *Analyst* **2020**, *145* (23), 7559−7570.
(39) He, L.; Liu, Y.; Mustapha, A.; Lin, M. Antifungal activity of zinc oxide nanoparticles against Botrytis cinerea and Penicillium expansum. *Microbiological research* **2011**, *166* (3), 207−215.
(40) Ebert, C.; Tuchscherr, L.; Unger, N.; Pöllath, C.; Gladigau, F.; Popp, J.; Löffler, B.; Neugebauer, U. Correlation of crystal violet biofilm test results of Staphylococcus aureus clinical isolates with Raman spectroscopic read-out. *J. Raman Spectrosc.* **2021**, *52* (12), 2660−2670.
(41) Sundaram, J.; Park, B.; Hinton, A.; Lawrence, K. C.; Kwon, Y. Detection and differentiation of Salmonella serotypes using surface enhanced Raman scattering (SERS) technique. *Journal of Food Measurement and Characterization* **2013**, *7*, 1−12.
(42) Kahraman, M.; Zamaleeva, A. I.; Fakhrullin, R. F.; Culha, M. Layer-by-layer coating of bacteria with noble metal nanoparticles for surface-enhanced Raman scattering. *Anal. Bioanal. Chem.* **2009**, *395* (8), 2559−2567.
(43) Efrima, S.; Zeiri, L. Understanding SERS of bacteria. *Journal of Raman Spectroscopy: An International Journal for Original Work in all Aspects of Raman Spectroscopy, Including Higher Order Processes, and also Brillouin and Rayleigh Scattering* **2009**, *40* (3), 277−288.
(44) Kengne-Momo, R.; Daniel, P.; Lagarde, F.; Jeyachandran, Y.; Pilard, J.; Durand-Thouand, M.; Thouand, G. Protein interactions investigated by the Raman spectroscopy for biosensor applications. *Int. J. Spectrosc.* **2012**, *2012*, No. 462901, DOI: 10.1155/2012/462901.
(45) Cheng, H.-W.; Luo, W.-Q.; Wen, G.-L.; Huan, S.-Y.; Shen, G.-L.; Yu, R.-Q. Surface-enhanced Raman scattering based detection of bacterial biomarker and potential surface reaction species. *Analyst* **2010**, *135* (11), 2993−3001.
(46) Movasaghi, Z.; Rehman, S.; Rehman, I. U. Raman spectroscopy of biological tissues. *Appl. Spectrosc. Rev.* **2007**, *42* (5), 493−541.
(47) Akanny, E.; Bonhommé, A.; Commun, C.; Doleans-Jordheim, A.; Farre, C.; Bessueille, F.; Bourgeois, S.; Bordes, C. Surface-enhanced Raman spectroscopy using uncoated gold nanoparticles for bacteria discrimination. *J. Raman Spectrosc.* **2020**, *51* (4), 619−629.
(48) Ur Rehman, I.; Movasaghi, Z.; Rehman, S. *Vibrational spectroscopy for tissue analysis*; CRC Press, 2012.
(49) Hamasha, K.; Sahana, M. B.; Jani, C.; Nyayapathy, S.; Kang, C.-M.; Rehse, S. J. The effect of Wag31 phosphorylation on the cells and the cell envelope fraction of wild-type and conditional mutants of Mycobacterium smegmatis studied by visible-wavelength Raman spectroscopy. *Biochemical and biophysical research communications* **2010**, *391* (1), 664−668.
(50) Sajan, D.; Sockalingum, G.; Manfait, M.; Hubert Joe, I.; Jayakumar, V. NIR-FT Raman, FT-IR and surface-enhanced Raman scattering spectra, with theoretical simulations on chloramphenicol. *Journal of Raman Spectroscopy: An International Journal for Original Work in all Aspects of Raman Spectroscopy, Including Higher Order Processes, and also Brillouin and Rayleigh Scattering* **2008**, *39* (12), 1772−1783.
(51) Tchobanoglous, G.; Burton, F.; Stensel, H. *Wastewater engineering treatment and reuse* (No. 628.3 T252s); McGraw-Hill Higher Education: Boston, US, 2003.
(52) Jung, G. B.; Nam, S. W.; Choi, S.; Lee, G.-J.; Park, H.-K. Evaluation of antibiotic effects on Pseudomonas aeruginosa biofilm using Raman spectroscopy and multivariate analysis. *Biomedical optics express* **2014**, *5* (9), 3238−3251.
(53) Hecker, M.; Völker, U. General stress response of Bacillus subtilis and other bacteria. *Advances in Microbial Physiology* **2001**, *44*, 35−91.
(54) Soni, D.; Bafana, A.; Gandhi, D.; Sivanesan, S.; Pandey, R. A. Stress response of Pseudomonas species to silver nanoparticles at the molecular level. *Environmental toxicology and chemistry* **2014**, *33* (9), 2126−2132.
(55) Wang, P.; Pang, S.; Zhang, H.; Fan, M.; He, L. Characterization of Lactococcus lactis response to ampicillin and ciprofloxacin using surface-enhanced Raman spectroscopy. *Anal. Bioanal. Chem.* **2016**, *408* (3), 933−941.
(56) Hayat, K.; Shkeel, M.; Iqbal, M. A.; Quah, C. K.; Wong, Q. A.; Nazari, M.; Ahamed, M. B. K.; Hameed, S. O-Halogen-substituted arene linked selenium-N-heterocyclic carbene compounds induce significant cytotoxicity: Crystal structures and molecular docking studies. *J. Organomet. Chem.* **2023**, *985*, No. 122593.
(57) Pavia, D. L.; Lampman, G. M.; Kriz, G. S.; Vyvyan, J. A. *Introduction to spectroscopy*; Cengage Learning: **2014**.
(58) Wu, X.; Huang, Y.-W.; Park, B.; Tripp, R. A.; Zhao, Y. Differentiation and classification of bacteria using vancomycin functionalized silver nanorods array based surface-enhanced Raman spectroscopy and chemometric analysis. *Talanta* **2015**, *139*, 96−103.
(59) Witkowska, E.; Korsak, D.; Kowalska, A.; Janeczek, A.; Kamińska, A. Strain-level typing and identification of bacteria−a novel approach for SERS active plasmonic nanostructures. *Anal. Bioanal. Chem.* **2018**, *410*, 5019−5031.
(60) Wu, X.; Xu, C.; Tripp, R. A.; Huang, Y.-W.; Zhao, Y. Detection and differentiation of foodborne pathogenic bacteria in mung bean sprouts using field deployable label-free SERS devices. *Analyst* **2013**, *138* (10), 3005−3012.

https://doi.org/10.1021/acsomega.3c08196
ACS Omega 2024, 9, 6861−6872